

A CYCLIC COHESIVE ZONE MODEL FOR TRANSIENT THERMOMECHANICAL LOADING

GRYGORIY KRAVCHENKO* AND HEINZ E. PETTERMANN†

* Institute of Lightweight Design and Structural Biomechanics (ILSB)
Vienna University of Technology
Gusshausstrasse 27-29, 1040 Vienna, Austria
e-mail: kravchen@ilsb.tuwien.ac.at, web page: <http://www.ilsb.tuwien.ac.at/>

† e-mail: pettermann@ilsb.tuwien.ac.at, web page: <http://www.ilsb.tuwien.ac.at/>

Key words: Fatigue crack growth, cohesive zone model, thermomechanical loading, transient conditions.

Abstract. A cyclic cohesive zone model based on a damage evolution equation is extended onto a case of transient thermal loading conditions. The thermomechanical extension is realised by augmenting mechanical relations with relations for thermal flux across the cohesive zone for both open and closed crack states. The model is also extended onto the case of anisothermal fatigue by incorporating temperature dependence of the cohesive zone model parameters. Furthermore, a cycle jump technique based on the direct iteration of the damage evolution equation is implemented and utilised to speed-up the fatigue simulations. A finite element analysis of fatigue crack growth at an interface of a bilayer structure under pulsing thermal loading is carried out and discussed in detail.

1 INTRODUCTION

The cohesive zone modelling approach is a powerful tool which allows to describe formation and propagation of cracks for a wide range of problems involving materials with nonlinear properties, materials interfaces, coupled problems, etc. Over the last years, the cohesive zone approach was also widely adopted for modelling fatigue cracking in structures subjected to cyclic loading. The approach is based on an idea of incorporating hysteresis into the unloading-reloading cohesive zone response, permitting to model damage accumulation process on a cycle-by-cycle basis [1–3]. Recently, the cyclic cohesive zone models (CZMs) were also extended onto problems involving creep-fatigue [4] and creep-fatigue with oxidation-assisted cracking [5].

In parts subjected to thermomechanical cyclic loading, especially with large temperature gradients, the fatigue crack formation and growth may additionally be altered by

redistribution of the coupled thermomechanical fields caused by degradation of thermal conductance across the damaged zone as well as by the thermal contact of newly formed crack faces. To model the described behaviour, a coupling between the thermal and the mechanical fields must be included into a CZM. Such extensions onto the thermomechanical problems can be achieved by augmenting the mechanical relations with relations for thermal flux, as was demonstrated for monotonic and cyclic CZMs [6–8]. In these models, the thermal and mechanical fields are coupled via a single damage variable which controls reduction of peak traction or stiffness and thermal conductance of the cohesive zone in a unified fashion.

Another important aspect is temperature dependence of various damage mechanisms. Therefore, for successful application of thermomechanical CZMs to problems involving anisothermal loading conditions, temperature dependence of CZM parameters has to be implemented as well. Such implementation was proposed in [6], where the cohesive strength was assumed to be linearly temperature dependent. In [9], temperature dependence of the cohesive stiffness and the fracture energy was incorporated into a cyclic CZM that was applied to modelling fatigue failure in solder joints of power electronic modules subjected to passive thermal cycling.

In this contribution, a cyclic CZM proposed in [4] is extended onto a case of fatigue crack growth (FCG) under transient nonisothermal loading conditions. The thermal extension is realised by augmenting mechanical relations with relations for thermal flux across the cohesive zone, along similar considerations as proposed in [6, 7]. The implemented thermomechanical CZM allows to describe evolving tractions and heat flux across the cohesive zone both in open and closed states. Furthermore, the model is extended onto anisothermal cases by considering temperature dependence of the CZM parameters. To accelerate the FCG simulations, the implementation also includes a cycle jump technique based on direct iteration of the damage evolution equation, as suggested in [10]. An analysis of FCG at an interface of a bilayer structure under pulsing transient thermal load using the finite element method (FEM) is presented and discussed in detail.

2 THERMOMECHANICAL CYCLIC COHESIVE ZONE MODEL

2.1 Load transfer

For completeness, the main features of the cyclic CZM presented in [4] are outlined below. In this model, the normal and tangential cohesive tractions (T_N , T_T) are assumed to be linear functions of the corresponding separation components (U_N , U_T):

$$T_N = K_N(1 - D) \frac{\langle U_N \rangle}{\delta_c} \quad (1)$$

$$T_T = \alpha K_N(1 - D) \frac{U_T}{\delta_c}, \quad \alpha = \frac{K_T}{K_N}, \quad (2)$$

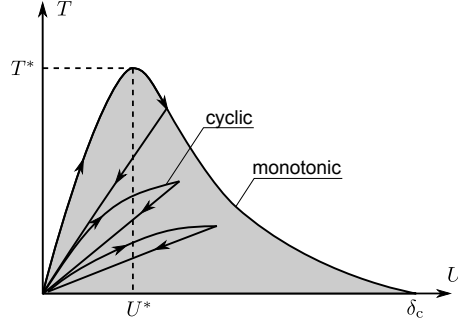


Figure 1: Schematic representation of a hysteretic traction-separation law.

where D is the damage variable used to characterise reduction of the cohesive zone stiffness, K_N and K_T is the normal and the tangential cohesive zone stiffness, α is the stiffness ratio and δ_c is the critical separation. The symbol $\langle \cdot \rangle$ denotes the Macauley's brackets.

The damage variable is computed using the following damage evolution equation:

$$\dot{D} = A^*(1 - D)^m \left\langle \frac{\|T\|}{1 - D} - T_0 \right\rangle^n \|\dot{U}\| \quad (3)$$

where T_0 is the traction threshold, A^* , m , n are the CZM constants (eventually, temperature dependent), $\|U\|$ and $\|T\|$ are the effective traction and separation, respectively, defined by the following relations:

$$\|U\| = \sqrt{\left(\frac{\langle U_N \rangle}{\delta_c}\right)^2 + \alpha \left(\frac{U_T}{\delta_c}\right)^2} \quad (4)$$

$$\|T\| = \sqrt{\langle T_N \rangle^2 + \frac{1}{\alpha} T_T^2} \quad (5)$$

In equation (3) the damage accumulation $\dot{D} > 0$ occurs only on loading when $\|\dot{U}\| > 0$.

As illustrated in figure 1, the cyclic traction-separation behaviour is intrinsically hysteretic and does not follow a predefined path, which is usually the case with CZMs for monotonic loading.

The case of crack closure and contact is modelled using the penalty based approach. For penetration ($U_N < 0$), the normal traction is calculated using the penalty stiffness K_c :

$$T_N = K_c \frac{U_N}{\delta_c} \quad (6)$$

The contact is assumed to be frictionless.

2.2 Heat transfer

The heat flow in the cohesive zone is assumed to occur only in normal direction. Denoting the opposite cohesive zone surfaces by subscripts 1 and 2, the thermal flux out of the surface with subscript “1” (positive flowing out), is given by:

$$q_1 = h_{cz}(\theta_1 - \theta_2) \quad (7)$$

where θ_i ($i = 1, 2$) is the absolute temperature of the respective cohesive surface and h_{cz} is the thermal conductance across the cohesive zone. The temperature jump $\Delta\theta_{cz}$ across the cohesive zone and the average temperature of the cohesive zone θ_{cz} are defined, as follows:

$$\Delta\theta_{cz} = \theta_1 - \theta_2, \quad \theta_{cz} = (\theta_1 + \theta_2)/2$$

Following the work presented in [6], the thermal conductance across the cohesive zone on opening is assumed to be proportional to the undamaged fraction of the CZ, represented by $(1 - D)$. Neglecting heat transfer by convection and radiation, the thermal conductance in this case is:

$$h_{cz} = (1 - D)h_{\text{int}}, \quad U_N \geq 0, \quad (8)$$

where h_{int} is the thermal conductance of the undamaged interface. Assuming the presence of external heat sources of high intensity, heat generation due to the damage process is neglected.

On closure, the heat transfer occurs through the undamaged part of the cohesive zone and through the cohesive zone surfaces in contact. In this case, the thermal conductance is given by [7]:

$$h_{cz} = (1 - D)h_{\text{int}} + Dh_c, \quad U_N < 0 \quad (9)$$

where h_c is the thermal conductance across the cohesive zone surfaces in contact.

For a case of elastic contact, the thermal contact conductance can be estimated from [11, 12]:

$$h_c = \frac{2k_1k_2}{E^*(k_1 + k_2)} \frac{\partial p}{\partial w_I} \quad (10)$$

where

$$\frac{1}{E^*} = \frac{(1 - \nu_1^2)}{E_1} + \frac{(1 - \nu_2^2)}{E_2} \quad (11)$$

is the composite elastic compliance of the contacting bodies, E_i is the Young’s modulus, ν_i

is the Poisson's ratio, k_i is the thermal conductivity of the respective material ($i = 1, 2$), p is the contact pressure and w_I is the normal gap.

Generally, the local contact pressure, and thus the thermal contact conductance, strongly depend on surface roughness of the contacting bodies. In this work, however, the effect of surface roughness was neglected and for the penalty based approach the incremental interface stiffness $\partial p / \partial w_I$ reduces to the penalty contact stiffness:

$$\frac{\partial p}{\partial w_I} = \frac{\partial T_N}{\partial U_N} = K_c, \quad U_N < 0.$$

Evidently, choosing higher values of K_c results in proportionally higher values of h_c (see equation (10)). To obtain physically more realistic estimations, use of nonlinear pressure-overclosure relationships, such as an exponential or a power-law type, would be more advantageous.

2.3 Cycle jump technique

For a large number of cycles e.g., 10^4 and more, simulation of FCG on a cycle-by-cycle basis would require a large number of computation increments which results in prohibitively large simulation time. To circumvent this problem, the so-called ‘‘cycle jump’’ technique based on damage extrapolation is widely used in engineering calculations. In context of FCG simulations using the cohesive zone modelling approach, linear and logarithmic extrapolation schemes have been proposed in [13] and [10]. To eliminate the need to make assumptions about the form (linear, logarithmic or else) of damage evolution, an approach based on direct iteration of the damage evolution equation can be utilised [10]. In this approach, the damage evolution equation (3) is iterated the number of jump cycles ΔN , giving a damage increment ΔD at the end of the cycle jump. Assuming steady state periodic loading conditions, the number of jump cycles in the next simulated cycle can be estimated from

$$\Delta N_{i+1} = \frac{\Delta D_{\text{allow}}}{\Delta D_{i,\text{max}}} \Delta N_i \tag{12}$$

where ΔD_{allow} is the allowed damage increment per load substep (or load increment), $\Delta D_{i,\text{max}}$ is the maximum damage increment per load substep which occurred at some integration point during the previous simulated cycle with a cycle jump ΔN_i . Evidently, smaller values of ΔD_{allow} result in better accuracy but longer simulation times. The value $\Delta D_{\text{allow}} = 0.01$ proved to be a good compromise between results accuracy and simulation time.

To avoid situations when $\Delta D_{i,\text{max}}$ substantially exceeds ΔD_{allow} due to sudden increase of ΔN_{i+1} compared to ΔN_i , the following expression with a more conservative cycle jump

increase can be used:

$$\Delta N_{i+1} = \Delta N_i + \lambda(\Delta N_{i+1} - \Delta N_i), \quad \Delta N_{i+1} > \Delta N_i \quad (13)$$

where $\lambda \in [0, 1]$ is a coefficient “damping” the increase of jump cycles between two consecutive simulated cycles. $\lambda = 0.5$ proved to be a reasonable value.

2.4 Implementation aspects

The thermomechanical cyclic CZM was implemented into the commercially available finite element method software ANSYS® by means of USERINTER user contact subroutine. The implementation contains the following tangent interface stiffness matrix [14]:

$$\mathbf{K}_{cz} = \begin{bmatrix} \mathbf{K}_m & \mathbf{K}_{mt} \\ \mathbf{K}_{tm} & \mathbf{K}_{th} \end{bmatrix} \quad (14)$$

where the submatrix \mathbf{K}_m represents the mechanical coupling terms, the submatrices \mathbf{K}_{mt} and \mathbf{K}_{tm} represent the mechanical-thermal and the thermal-mechanical coupling terms, respectively. The thermal coupling terms are represented by the submatrix \mathbf{K}_{th} . The assumptions for the thermomechanical interactions made in the previous sections lead to symmetric submatrices.

3 FATIGUE CRACK GROWTH IN A BILAYER STRUCTURE

3.1 Model description

The bilayer structure and boundary conditions (BCs) used in the simulations are schematically depicted in figure 2. The thickness and length of each layer is taken equal $10 \mu\text{m}$ and $50 \mu\text{m}$, respectively. The contact elements for modelling the cohesive zone behaviour are located between the layers and an edge pre-crack of length $a_0 = 10 \mu\text{m}$ is inserted at the layers interface on the left side. The structure is loaded cyclically by a pulsing thermal flux $q_{\text{pulse}} = 100 \text{ W/mm}^2$ of duration $t_{\text{pulse}} = 80 \mu\text{s}$ applied at the bottom, which is followed by a shutdown period of $160 \mu\text{s}$. The convective cooling with a film coefficient $h_{\text{conv}} = 1 \text{ W/(mm}^2 \text{ K)}$ and the sink temperature $\theta_{\text{sink}} = 358 \text{ K}$ is applied at the top. The left and right sides of the structure are assumed to be perfectly insulated. The initial temperature is assumed to be equal the temperature of the sink. The bottom and right sides of the structure are constrained in vertical and horizontal directions, respectively, as shown in the figure.

The thermal and elastic properties of the layers are assumed to be isotropic temperature independent, as listed in table 1. The reference (stress-free) temperature of both layers is taken equal $\theta_{\text{ref}} = 458 \text{ K}$.

The simulations were carried out with assumed CZM parameters, chosen to represent the Paris regime [15] of FCG, as pointed out in [4]. The temperature independent param-

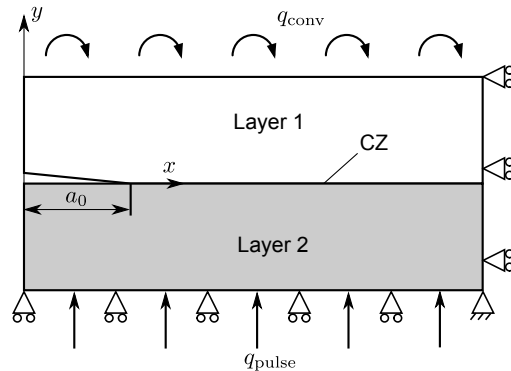


Figure 2: Schematic representation of the bilayer structure and boundary conditions.

Table 1: Thermal and elastic properties of the bilayer constituents.

Layer	k W/(m K)	C_p J/(kg K)	ρ kg/m ³	E GPa	ν	α (CTE) 10 ⁻⁶ /K
1	385.0	385	8960	110	0.35	16.4
2	38.5	770	2970	160	0.26	4.1

eters were chosen, as follows: $K_N = 5 \times 10^9$ MPa, $\alpha = 0.5$ (stiffness ratio), $T_0 = 1$ MPa, $\delta_c = 10^{-5}$ mm, $K_c = K_N$. Further CZM parameters were assumed to be temperature-dependent and are summarised in table 2. Furthermore, to avoid significant thermal field disturbance across the intact CZ, the interface thermal conductance was taken equal $h_{\text{int}} = 5 \times 10^3$ W/(mm² K). The thermal simulations performed under the above described conditions showed that a temperature jump of less than 0.1 K is introduced in this way.

Table 2: Temperature dependent cyclic CZM parameters.

θ K	m	n	A^* mm ⁻¹ MPa ⁻ⁿ
358	1.80	1.50	8.88×10^{-7}
408	1.71	1.62	1.30×10^{-6}
458	1.58	1.70	1.83×10^{-6}
508	1.44	1.74	2.17×10^{-6}
558	1.26	1.77	2.35×10^{-6}
608	1.04	1.80	2.53×10^{-6}

The layers were meshed with coupled thermal-structural two-dimensional isoparametric elements with linear shape functions. The mesh was refined near the simulated crack propagation path with the element length in this region being equal about 0.03 μm . The interface between the layers representing the cohesive zone was meshed with contact elements. Plane strain conditions were assumed in the model.

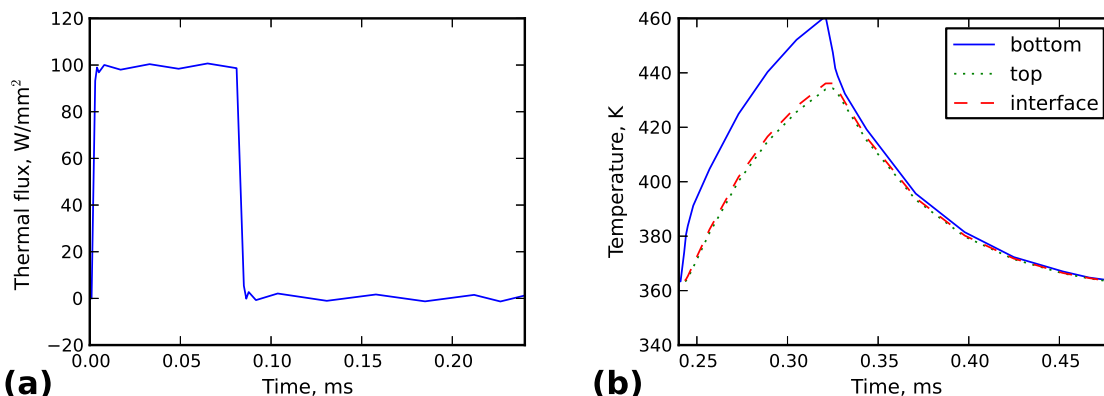


Figure 3: (a) Evolution of thermal flux at the bottom of the bilayer; (b) evolution of temperature in the region unaffected by the crack during a thermally stabilised cycle.

4 Results

The pulsing thermal flux applied at the bottom of the bilayer structure, presented in figure 3a, results in temperature rise and subsequent cooldown due to convective cooling applied at the top. Figure 3b shows evolution of temperature at the bottom, top and interface of the bilayer structure during the second cycle for the right side of the structure, which is not affected by the crack yet. The temperature swing in this region for the top layer is about 80 K. As can be noted, a periodic steady state is already achieved in the second cycle.

The damage accumulated in the cohesive zone after about 1×10^4 cycles is presented in figure 4a. At this time instance, 8 elements are damaged completely and do not transfer tractions and heat across the cohesive zone on opening. Also corresponding to this number of cycles, the figure 4b shows the distribution of the thermal flux across the cohesive zone at the end of the heating phase. Assuming the crack tip is located at the point of maximum flux (or tractions), as proposed in [16], the wake and the forward ($D > 0.1$) regions count 6 and 8 elements, respectively. Note that the actual forward region is much longer in case $D > 0$ condition is assumed. This is due to a low chosen value of $T_0 = 1$ MPa, which results in damage accumulation (although very small) in every cycle even at locations far ahead of the crack tip.

Figure 5a demonstrates evolution of damage and thermal conductance on opening at the location $x = a_0 + 0.3 \mu\text{m}$ plotted for the first 6×10^3 cycles. Evidently, the “mirror” symmetric behaviour of both curves is the consequence of equation (8). The damage accumulation rate is not constant and can be divided roughly in three stages. During the first stage, when the crack tip is far enough from the observed location, the damage accumulation rate is low but slowly increasing. This stage is attributed to the forward region. The second stage can be characterised by significantly increased damage accumulation rates when the crack tip approaches and passes through the observed location. Finally,

during the third stage the damage accumulation rate is again low approaching zero, when the observed location is in the wake region. The fracture process zone (FPZ) size and the form of the damage evolution curve under the prescribed loading depend on the choice of the CZM parameters.

Corresponding to the above discussed location, figure 5b presents the evolution of maximum temperature jump across the cohesive zone, corresponding to the end of the heating phase. One can observe that up to 4×10^3 cycles the temperature jump is negligible starting to increase rapidly when $D \approx 0.5$. By the end of 1×10^4 cycles the temperature jump reaches about 10 K which is a substantial increase compared to a temperature swing of about 80 K, observed earlier from figure 3b. Further crack propagation would obviously result in a larger temperature jump but is omitted in this discussion.

The crack growth rate (CGR) plotted as a function of number of cycles is presented in figure 6. In calculations of the CGR, the crack tip was assumed to be at the location of maximum tractions, as mentioned above. Note that the initial much higher CGR is attributed to a not completely developed FPZ in the model when damage accumulation mostly occurs in the first several elements ahead of the pre-crack. For correct interpretation of the results this stage should be ignored. The cohesive zone can be considered to be fully developed only after formation of the wake region, (controlled by the parameter m), which occurs after these first several elements have accumulated a significant amount of damage. The simulation results show that the CGR stabilizes after about 1.5×10^4 cycles at a value of 1×10^{-7} mm/cycle. It also may be noted that the increasing CGR prior to the stabilisation is due to a slow development of the forward zone (controlled by T_0).

5 CONCLUSIONS

This contribution presented a thermomechanical cyclic CZM that can be applied to model fatigue crack propagation under transient thermal loading conditions. The contact implementation of the model allows to describe thermomechanical interaction of the

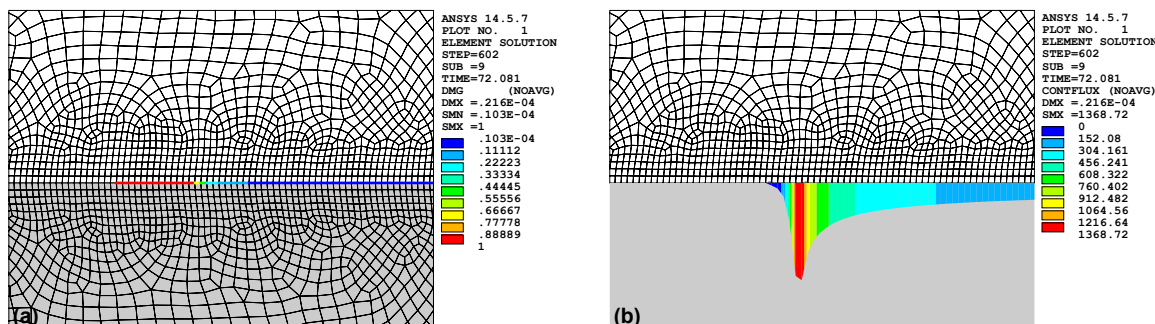


Figure 4: Distribution of (a) damage and (b) the thermal flux (end of the heating phase) in the cohesive zone after about 1×10^4 cycles. For interpretation of the plots please refer to the colour version of this article.

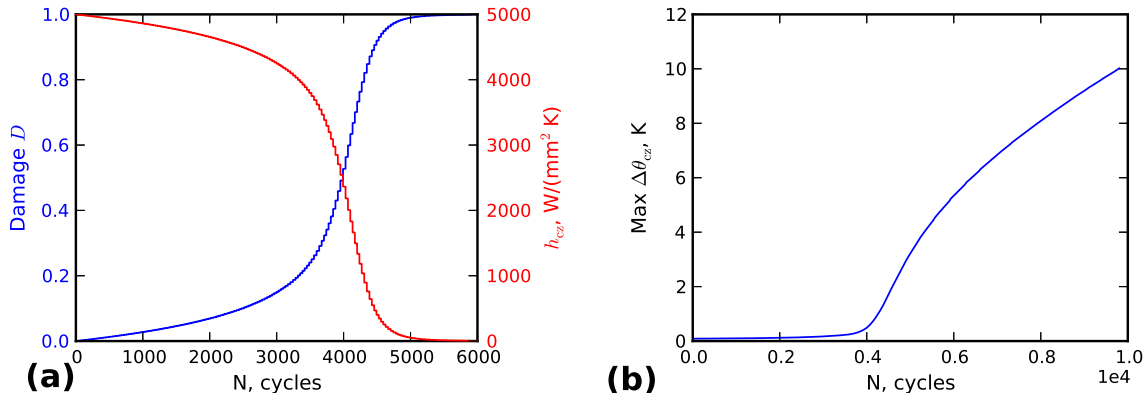


Figure 5: Evolution of (a) damage and thermal conductance across the CZ; (b) maximum temperature jump across the cohesive zone. The results are extracted for the location $x = a_0 + 0.3 \mu\text{m}$

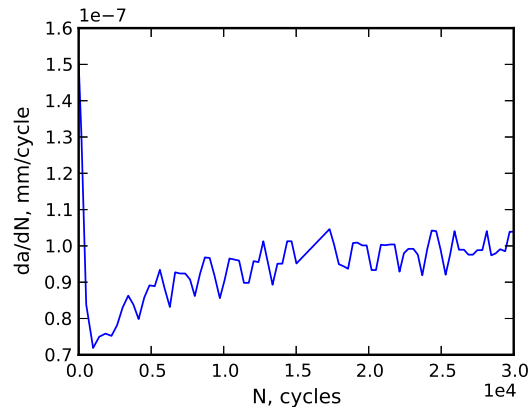


Figure 6: Crack growth rate as a function of number of cycles.

cohesive surfaces in both open and closed states. Furthermore, an important aspect of temperature dependence of the cohesive zone parameters is considered as well, extending applicability of the model onto cases of anisothermal fatigue. The implementation also incorporates the cycle jump technique based on direct iteration of the damage evolution equation which can greatly speed-up fatigue simulations without sacrificing results accuracy. Finally, the application of the implemented CZM was demonstrated on a problem of fatigue crack growth at the interface of a bilayer structure subjected to pulsing thermal loading followed by a detailed discussion of the simulation results.

ACKNOWLEDGEMENTS

This work was jointly funded by the Austrian Research Promotion Agency (FFG, Project No. 831163) and the Carinthian Economic Promotion Fund (KWF, contract KWF-1521-22741-34186).

References

- [1] O. Nguyen, E. Repetto, M. Ortiz, and R. Radovitzky, “A cohesive model of fatigue crack growth,” *International Journal of Fracture*, vol. 110, pp. 351–369, 2001.
- [2] B. Yang, S. Mall, and K. Ravi-Chandar, “A cohesive zone model for fatigue crack growth in quasibrittle materials,” *International Journal of Solids and Structures*, vol. 38, pp. 3927 – 3944, 2001.
- [3] K. Roe and T. Siegmund, “An irreversible cohesive zone model for interface fatigue crack growth simulation,” *Engineering Fracture Mechanics*, vol. 70, pp. 209 – 232, 2003.
- [4] J. Bouvard, J. Chaboche, F. Feyel, and F. Gallerneau, “A cohesive zone model for fatigue and creep-fatigue crack growth in single crystal superalloys,” *International Journal of Fatigue*, vol. 31, pp. 868–879, 2009.
- [5] Y. Sun, K. Maciejewski, and H. Ghonem, “A damage-based cohesive zone model of intergranular crack growth in a nickel-based superalloy,” *International Journal of Damage Mechanics*, vol. 22, no. 6, pp. 905–923, 2013.
- [6] A. Hattiangadi and T. Siegmund, “A numerical study on interface crack growth under heat flux loading,” *International Journal of Solids and Structures*, vol. 42, pp. 6335 – 6355, 2005.
- [7] I. Oezdemir, W. Brekelmans, and M. Geers, “A thermo-mechanical cohesive zone model,” *Computational Mechanics*, vol. 46, pp. 735–745, 2010.
- [8] A. Hattiangadi and T. Siegmund, “An analysis of the delamination of an environmental protection coating under cyclic heat loads,” *European Journal of Mechanics - A/Solids*, vol. 24, no. 3, pp. 361 – 370, 2005.
- [9] Z. Sun, L. Benabou, and P. Dahoo, “Prediction of thermo-mechanical fatigue for solder joints in power electronics modules under passive temperature cycling,” *Engineering Fracture Mechanics*, vol. 107, pp. 48 – 60, 2013.
- [10] A. Ural and K. D. Papoulia, “Modeling of fatigue crack growth with a damage based cohesive zone model,” in *ECCOMAS European Congress on Computational Methods in Applied Sciences and Engineering* (P. Neittaanmäki, T. Rossi, K. Majava, and O. Pironneau, eds.), July 2004.
- [11] J. Barber, “Bounds on the electrical resistance between contacting elastic rough bodies,” *Proceedings of the Royal Society of London. Series A: Mathematical, Physical and Engineering Sciences*, vol. 459, no. 2029, pp. 53–66, 2003.

- [12] J. Barber, “Incremental stiffness and electrical contact conductance in the contact of rough finite bodies,” *Physical Review E - Statistical, Nonlinear, and Soft Matter Physics*, vol. 87, no. 1, pp. 013203–5, 2013.
- [13] A. de Andres, J. Perez, and M. Ortiz, “Elastoplastic finite element analysis of three-dimensional fatigue crack growth in aluminum shafts subjected to axial loading,” *International Journal of Solids and Structures*, vol. 36, pp. 2231 – 2258, 1999.
- [14] ANSYS, Inc., “ANSYS Academic Research, Release 14.5, Help System, Programmer’s Reference,” 2012.
- [15] P. C. Paris, M. P. Gomez, and W. E. Anderson, “A rational analytic theory of fatigue,” *The trend in engineering*, vol. 13, pp. 9–14, 1961.
- [16] H. Li and N. Chandra, “Analysis of crack growth and crack-tip plasticity in ductile materials using cohesive zone models,” *International Journal of Plasticity*, vol. 19, pp. 849 – 882, 2003.